République Algérienne Démocratique et Populaire

وزارة التعليم العالي والبحث العلمي

Ministère de l'Enseignement Supérieur et de la Recherche Scientifique

Université Bordj Bou Arreridj

Faculté des Sciences et de la Technologie

Department Sciences de la Matière

جامعة برج بوعريريج

كلية العلوم والتكنولوجيا

قسم علوم المادة

Mémoire de fin d'étude

PRESENTÉ EN VUE DE L'OBTENTION

DU DIPLOME DE : **Master**

Filière : **physique**

Option : **physique des Matériaux**

THÈME:

Solution du modèle de Cohen Bergstresser pour le silicium

Préparé par :

Siassi Abderrahim

Soutenu le **: 20/09/2020**

Devant le jury :

Président :	*N. Benchiheub*	*MCB*	*Université de Bordj Bou Arreridj*
Rapporteur :	*N. Grar*	*MCA*	*Université de Bordj Bou Arreridj*
Examinateur :	*N. Lebga*	*MCB*	*Université de Bordj Bou Arreridj*
Examinateur :	*A. Benthabet*	*PR*	*Université de Bordj Bou Arreridj*

Année Universitaire 2019-2020

Acknowledgments

First, I would like to thank god for his help, his forgiveness, and his charity. I would also like to thank my dear parents. Furthermore, I would like to express my gratitude to my supervisor Dr N. Grar for the useful comments, remarks and engagement through the learning process of this master thesis. In addition, I would like to thank the committee members. I would like to say to all my teachers at this university "thank you very much". At last, I would like to thank my dear friend Jacob for his help.

I would like to dedicate this work to all my dear family and friends, especially Jacob, Khaoula, Oussama, Islam, Oussama, Jacov, Ibrahim, Zaki.

Abstract

The electronic band structure calculation for semi-conductors is very helpful in knowing their proprieties. In this thesis, the electronic band structure for 3 diamond structures crystals: Silicon (Si), Germanium (Ge), Tin (Sn), and 3 zincblende structure: Aluminum antimonide (AlSb) , Gallium phosphide (GaP) , Gallium arsenide (GaAs) is calculated . We choose to use the Empirical Pseudopotential Method with the same model adopted by Cohen and bergstresser. The model is coded using Fortran programing language and the diagonaliztion is elaborated using LAPACK libraries.

Résumé

Le calcul de la structure de bande électronique pour les semi-conducteurs est très utile pour connaître leurs caractéristiques. Dans cette thèse, la structure de bande électronique pour 3 cristaux de structures de diamant : Silicium (Si), Germanium (Ge), Étain (Sn), et 3 structures de zincblende : Antimoniure d'aluminium (AlSb), Phosphure de Gallium (GaP), Arséniure de Gallium (GaAs) est calculée. Nous choisissons d'utiliser la méthode pseudopotentielle empirique avec le même modèle adopté par Cohen et bergstresser. Le modèle est codé à l'aide du langage de programmation Fortran et la diagonale est élaborée à l'aide des bibliothèques LAPACK.

نبذة مختصرة

حساب هيكل النطاق الالكتروني لأشباه الموصلات مفيد جدا لمعرفة خصائصها. في هذه الأطروحة، نحاول حساب بنية النطاق الالكتروني لثلاث مواد بلورية ذات بنية ماسية و هي : السيليكون ، الجرمانيوم ، و القصدير ، و ثلاث مواد ذات بنية تشبه بنية السفاليريت و هي : اثميد الالمنيوم ، فوسفيد الجاليوم ، و زرنيخيد الجاليوم . اخترنا لهذا الغرض، اسلوب الكمون الزائف التجريبي مع اعتماد نفس النموذج المعتمد من طرف كوهن و بيرغسترسر ، البرنامج المستعمل للحساب تمت كتابته باستعمال لغة البرمجة Fortran والاستعانة بمكتبة الجبر الخطي LAPACK .

Content

Introduction

Semi-conductors nowadays are the most active and exciting research area. Indeed semiconductors are the most interesting materials ever discovered by humans. They are the heart of the modern world, due to their characteristics and properties which made them very useful in the technological industry. It is hard to find an integrated circuit or a modern device that is not based on semiconductors. This revolution starts in 1947, when the bipolar junction transistor first was invented, which opened new doors for the electronics industry and helps to improve the ability of devices like computers and cell phones. They can also be used in optoelectronic applications; diodes for example which are made of a PN junction are useful in light emission and reception in form of LED. Plenty of other applications can be given and upon which number of industries are built. Consequently it is necessary to study the properties of semiconductors and determine how they behave in deferent conditions. One of the most interesting properties of metals and semiconductors is the electronic band structure. Knowing the band structure of metals or semiconductors helps us to understand how the transport of electrons happens in devices made from those materials. It also helps in relating optical and electronic properties .

In order to calculate the electronic band structure, there are two basic approaches: “ab initio” and the empirical methods. Ab initio, or “from the beginning" methods involve calculation of band structure by use of first principles without using measured data. Empirical methods take advantage of experimental data to give more accurate band structure representation. Generally, ab initio methods are very intensive calculations but give better insight on how the structure is built. Both methods have their place in calculating and engineering transport properties in semiconductor devices. In this master project however, we are interested only in the empirical methods, especially the empirical pseudopotential method which is noted as EPM.

The pseudopotential term was first introduced by Fermi to study high-lying atomic states. Afterwards, Hellman proposed that pseudopotentials can be used for calculating the energy levels of the alkali metals. The wide spread usage of pseudopotentials did not occur until the late 1950s , when the research in condensed matter area began to accelerate. The main advantage of the previously mentioned method is that only valence electrons have to be considered, the core electrons are treated as if they are frozen in an atomic-like configuration.

As a result, the valence electrons are thought to move in a weak one electron potential. It also gives surprisingly accurate results considering the computing time and involved effort.

We are interested in this project by reviewing the psodeupotential approach, establishing the model that capture the main concepts. Afterwards the model is coded using Fortran language. The aim from one end is to show the simplicity of such a task using Lapack libraries and from another end is to prove the effectiveness of such an approach in the case of several semiconductors. It can be argued that such an approach is quite overtaken by all the details given by the ab initio calculations, however it is easy to understand the power of this approach when we notice that even in the framework of ab initio models, pseudopential approach is unavoidable in order to make the calculations tractable.

Our master report is accordingly organized as follows:

-In a first chapter we revisit the most important concepts of semiconductors, concepts that are important to understand the coming progression of our work.

-In a second chapter we develop the theoretical framework of the pseudopotential approach.

-In the third chapter we present our coding of the theoretical model. An evaluation of the program in different cases, reached results as well as our comments are also detailed.

- In a final conclusion we summarize the main scope of the work and the most important established results.

Chapter 1: Structures and Lattices

1.1. Introduction

Dealing with semiconductors lead us unavoidably to expose the main basis of solid state physics. In fact the crystalline structure of semiconductors are regular patterns that have several features in common. We are going to expose some of those features as an introductive part for the pseudopotential approach.

1.2. Crystalline structure

Crystalline structure is a description of the ordered arrangement of atoms, ions or molecules in a crystalline material. Ordered structures occur from the intrinsic nature of the constituent particles to form symmetric patterns that repeat along the principal directions of three dimensional space in matter. The unit cell of the structure is the smallest group of particles in the material that constitutes this repeated symmetrical pattern. It completely reflects the symmetry and structure of the entire crystal, which is built up by repetitive translation of the unit cell along its principal axes. The lengths of the principal axes of the unit cell and the angles between them are called lattice constants.

The positions and types of atoms in the primitive cell are called the basis. The set of translations, which generates the entire periodic crystal by repeating the basis, is a lattice of points in space called the Bravais lattice. So a crystal is defined by:

Crystal structure = Bravais lattice +basis

The Bravais lattice gives the well known patterns as cubic, body centered cubic, face centered cubic, diamond...structures.

The crystalline order is described by its symmetry operations. The set of translations forms a group because the sum of any two translations is another translation. In addition there may be other point operations that leave the crystal unchanged, such as rotations, reflections, and inversions. This can be summarized as[1]:

Space group = translation group + point group

1.2.1. The set of translation and the bravais lattice

The set of all translation forms the Bravais lattice in space, in which any translation can be defined by: $T(n) = \sum_{i=1}^{d} n_i a_i$,Where d is the dimension of the space, a_i are the primitive translations vectors, in three dimensions, the set of translations is written this way:

$$T(n) = n_1 a_1 + n_2 a_2 + n_3 a_3 \qquad (1.1)$$

These are the primitive vectors for some common Bravais lattice, (in units of a) [1]:

Face centered cubic (fcc) : $a_1 = \left(0, \frac{1}{2}, \frac{1}{2}\right)$, $a_2 = \left(\frac{1}{2}, 0, \frac{1}{2}\right)$, $a_3 = \left(\frac{1}{2}, \frac{1}{2}, 0\right)$

Body centered cubic (bcc): $a_1 = \left(-\frac{1}{2}, \frac{1}{2}, \frac{1}{2}\right)$, $a_2 = \left(\frac{1}{2}, -\frac{1}{2}, \frac{1}{2}\right)$, $a_3 = \left(\frac{1}{2}, \frac{1}{2}, -\frac{1}{2}\right)$ (1.2)

Simple cubic: $a_1 = (1,0,0)$, $a_2 = (0,1,0)$, $a_3 = (0,0,1)$

Simple hexagonal: $a_1 = (1,0,0)$, $a_2 = \left(\frac{1}{2}, \frac{\sqrt{3}}{2}, 0\right)$, $a_3 = \left(0,0, \frac{c}{a}\right)$

The fcc structure is shown in ***fig1.1***. The figure shows one possible choice of the primitive lattice vectors and the parallelepiped primitive cell, the wigner-seitz cell which is the first brillouin zone is also illustrated.

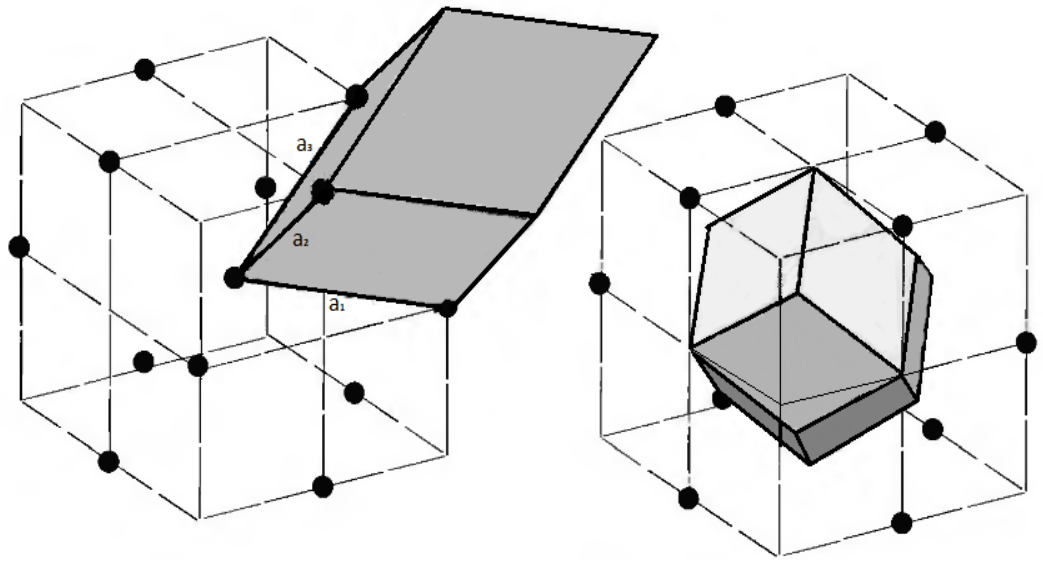

fig1.1: the fcc primitive cell and lattice vectors (left), the wigner-seitz cell for fcc(right).

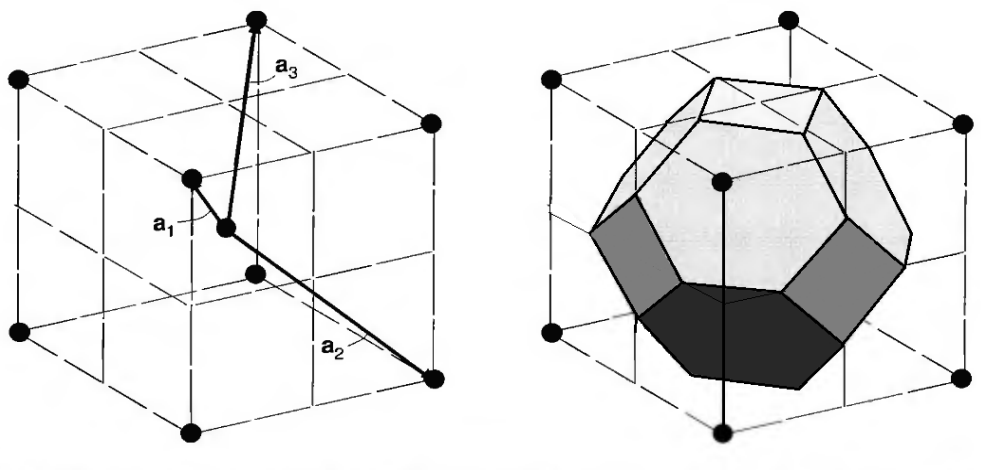

fig1.2: the bcc primitive cell and lattice vectors (left) ,the bcc Wigner Seitz cell (right) .

The volume of any primitive cell must be the same, since the translation of any such cell fill up all the space, so the most convenient choice of a cell in which to express the volume is the parallelepiped cell shown in ***fig1.1,*** the volume of the primitive cell defined by primitive vectors Ω_{cell} can be calculated this way:

$$\Omega_{cell} = |a_1 . (a_2 \times a_3)| \qquad (1.3)$$

1.2.2. Atom basis

The basis describes the position of atoms in each cell relative to a chosen origin, if there are *S* atoms per cell , then the basis of atoms is specified by the atomic position vectors τ_s, where *S* varies from 1 to *S*. We can also represent the atomic position vectors in terms of primitive lattice vectors *a*, they can be written this way [1]:

$$\tau_s = \sum_{i=1}^{d} \tau_{si}^{L} a_i \qquad (1.4)$$

Where *L* denotes the representation in lattice vectors, *d* is the dimension.

For our calculations, we are interested in the crystalline structure of silicon, which has diamond structure. The calculation are also carried in another step for the zincblende structure. Consequently we will study in some details those two structures.

1.2.2.1. Diamond structure

The diamond structure is fcc lattice constituted of two identical atoms per unit cell. Some common semiconductors have this structure such as silicon and germanium. A bond center is the appropriate choice of origin for the diamond structure since this is a center of inversion symmetry. By shifting the origin, the vectors are written this way (in units of a) [1]:

$$\tau_1 = -\left(\frac{1}{8}, \frac{1}{8}, \frac{1}{8}\right) \quad (1.5)$$

$$\tau_2 = \left(\frac{1}{8}, \frac{1}{8}, \frac{1}{8}\right)$$

in terms of primitive lattice vectors:

$$\tau_1^L = -\left[\frac{1}{8}, \frac{1}{8}, \frac{1}{8}\right] \quad (1.6)$$

$$\tau_2^L = \left[\frac{1}{8}, \frac{1}{8}, \frac{1}{8}\right]$$

1.2.2.2. Zincblende structure

The zincblende structure is the structure of many III-V and II-VI crystals such as GaAs and ZnS. This crystal is fcc lattice with two atoms per unit cell. Although there is no center of inversion in a zincblende structure crystal, each atom is at a center of tetrahedral symmetry [1]. Since the unit cell contains two non-identical atoms, we can place the origin at one atom, the atomic position vectors (in units of a) are:

$$\tau_1 = -\left(\frac{1}{8}, \frac{1}{8}, \frac{1}{8}\right) \quad (1.7)$$

$$\tau_2 = \left(\frac{1}{8}, \frac{1}{8}, \frac{1}{8}\right)$$

in terms of primitive lattice vectors , one can find that:

$$\tau_1^L = -\left[\frac{1}{8}, \frac{1}{8}, \frac{1}{8}\right] \quad (1.8)$$

$$\tau_2^L = \left[\frac{1}{8}, \frac{1}{8}, \frac{1}{8}\right]$$

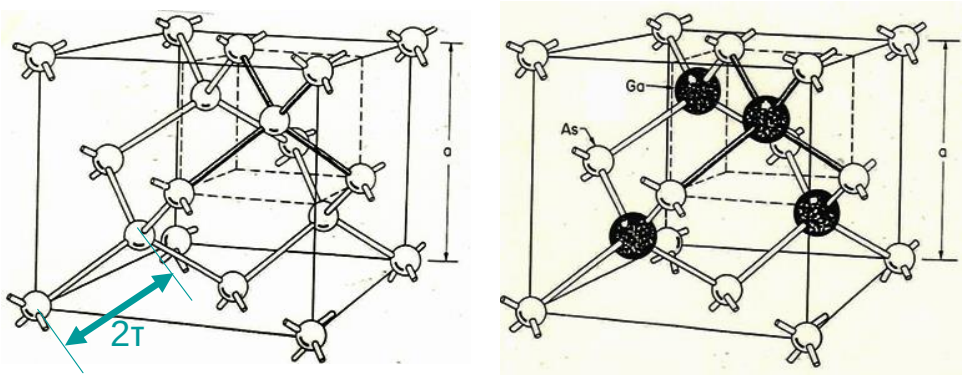

Diamond **Zincblende**

Si, Ge **GaAs**

fig 1.3 : the zincblende structure and diamond structure

1.3. Reciprocal lattice

The reciprocal lattice is the Fourier transform of the real Bravais lattice, the initial lattice (direct lattice) is a periodic spatial function in the real space. We can say that the reciprocal lattice is a representation of the real lattice in K-space (reciprocal space). The reciprocal of a reciprocal lattice is the original direct lattice.

1.3.1. Construction

consider any function $f(r)$ defined for the crystal (ex: the density of the electron) , which is the same in each unit cell , this means that :

$$f(r + T_n) = f(r) \qquad (1.9)$$

Where T_n can be any translation. Such a periodic function can be represented by Fourier transforms in terms of Fourier components at wavevectors q defined in reciprocal space. The formulas can be written most simply in terms of a discrete set of Fourier components if we restrict the Fourier components to those that are periodic in a large volume of crystal $\Omega_{crystal}$composed of N_{cell}[1]. then each component should satisfy the born-von Karmen boundary conditions in each dimension :

$$e^{iq.N_1a_1} = e^{iq.N_2a_2} = e^{iq.N_3a_3} = 1 \qquad (1.10)$$

Where N represents the number of unit cells in each direction.

So that q is restricted to the set of vector satisfying:

$$q.a_1 = 2\pi \frac{integer}{N_1}$$

$$q.a_2 = 2\pi \frac{integer}{N_2} \qquad (1.11)$$

$$q.a_3 = 2\pi \frac{integer}{N_3}$$

The final result should be independent from the particular choice of boundary conditions in the limit of large volume $\Omega_{crystal}$.

The Fourier transform is written this way:

$$f(q) = \frac{1}{\Omega_{crystal}} \int_{\Omega_{crystal}} \boldsymbol{d}r f(r)\, e^{iq.r} \qquad (1.12)$$

Which, for periodic functions, can be written :

$$f(q) = \frac{1}{N_{cell}} \sum_{n=1}^{d} e^{iq.T_n} \frac{1}{\Omega_{cell}} \int_{\Omega_{cell}} \boldsymbol{d}r f(r)\, e^{iq.r} \qquad (1.13)$$

The sum over all lattice points vanishes for all q except those that satisfy $q.T_n = 2\pi \times integer$ for all translations T. Since $T(n) = \sum_{i=1}^{d} n_i a_i$, we can write:

$$q.a_i = 2\pi \times integer \qquad (1.14)$$

The set of the Fourier components that satisfy this condition forms the reciprocal lattice , if we define the vectors b_i where i varies from 1 to d , that are reciprocal to the primitive translation vectors a_i , we can write :

$$b_i.a_j = 2\pi\delta_{ij} \qquad (1.15)$$

Where δ_{ij} is Kronecker symbol.

The only non-zero Fourier components for $f(r)$ are for , where the G vectors are a lattice of points in reciprocal space defined by :

$$G_m = \sum_{i=1}^{d} m_i b_i \qquad (1.16)$$

For each G , the Fourier transform of the periodic function can be written :

$$f(G) = \frac{1}{\Omega_{cell}} \int_{\Omega_{cell}} \boldsymbol{d}r f(r)\, e^{iG.r} \qquad (1.17)$$

The mutually reciprocal relation of the Bravais lattice in real space and the reciprocal lattice becomes apparent using matrix notation that is valid in any dimension. If we define the square matrix $b_{ij} = (b_i)_j$, then primitive vectors are related by :

$$b^T a = 2\pi \mathbf{1} \rightarrow b = 2\pi (a^T)^{-1} \qquad (1.18)$$

As a result, the reciprocal primitive vectors b_i can be calculated directly in terms of direct lattice vectors using the following equivalent expressions [1]:

$$b_1 = \frac{2\pi}{\Omega_{cell}} a_2 \times a_3$$

$$b_2 = \frac{2\pi}{\Omega_{cell}} a_3 \times a_1 \qquad (1.19)$$

$$b_3 = \frac{2\pi}{\Omega_{cell}} a_1 \times a_2$$

One can show that the reciprocal lattice of simple cubic structure is a simple cubic ,The cubic face centered and the cubic body centered are reciprocal to each other , the primitive vectors of reciprocal lattice for the cubic face centered lattice are given by (in units of $\frac{2\pi}{a}$):

$$b_1 = (-1\,, 1, 1)$$

$$b_2 = (1\,, -1, 1) \qquad (1.20)$$

$$b_3 = (1\,, 1, -1)$$

1.3.2. Brillouin zone:

The first brillouin zone is the Wigner-Seitz cell of the reciprocal lattice. The planes that are the perpendicular bisectors of the vectors from the origin to the reciprocal lattice points define the Wigner Seitz cell. The construction of the BZ of some common bravais lattices is illustrated in ***fig 1.4,*** and the widely used notations for points in the BZ of the face centered cubic are given in ***fig 1.5 .***

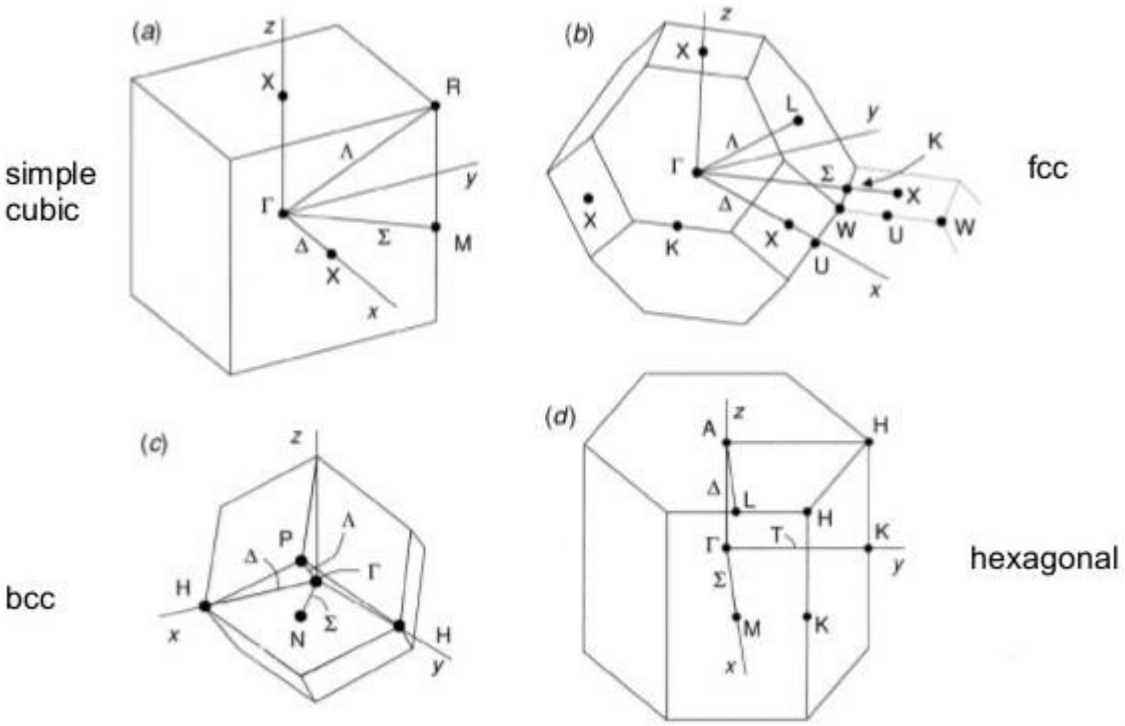

fig 1.4 : brillouin zone for some common bravais lattice and the widely used symmetry points for each zone

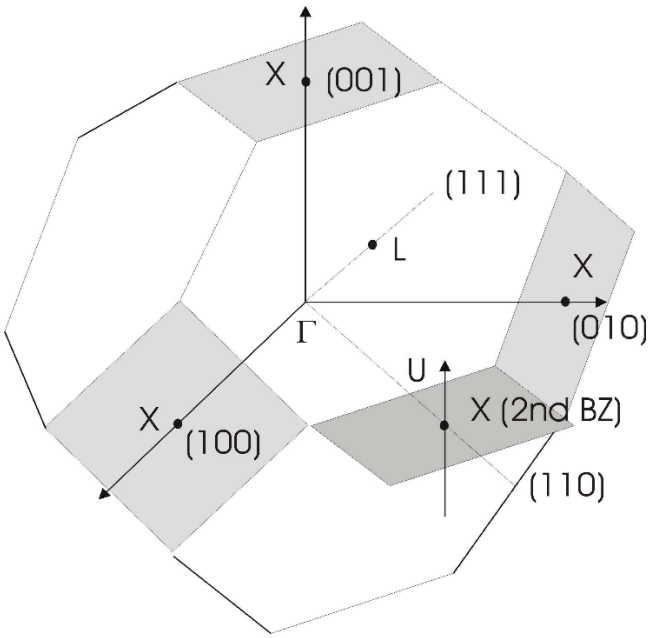

fig 1.5: high-symmetry points for the fcc lattice

High symmetry point and lines (shown in ***fig 1.4)*** are labeled according to Bouckaret, Smoluchowski, and Wigner [2]. The zone center (k =0) is designated Γ and interior lines by Greek letters, points on the zone boundary by Roman letters. In the case of the fcc lattice, a portion of a neighboring cell is represented by dotted lines. This shows the orientation of neighboring cells that provides useful information, for example that the line ∑ from Γ to K continues to a point outside the first BZ that is equivalent to X.

1.4. Periodic potential and Bloch theorem

The properties of an electron in a periodic potential can be described using Bloch's wave function, which have the following form:

$$\psi_k(r) = U_k(r)e^{ikr} \tag{1.21}$$

Where $U_k(r)$ is periodic ($U_k(r + T_n) = U_k(r)$), T_n could be any translation in the real space $T_n = n_1a_1 + n_2a_2 + n_3a_3$.

We can verify that Bloch function is an eigenfunction for the Hamiltonian with a periodic potential. To simplify things, we consider the one dimensional chain constituted of N atoms , with a lattice constant *a* , the Hamiltonian is given by :

$$\hat{H} = [\frac{-\hbar^2}{2m_0}\nabla^2 + V(x)] \tag{1.22}$$

Where $V(x)$ is the periodic potential:

$$V(x + a) = V(x) \tag{1.23}$$

Consider the translation operator $\hat{T}$, when $\hat{T}$ applied to $\psi_k(x)$ gives :

$$\hat{T}\psi_k(x) = \psi_k(x + a) \tag{1.24}$$

First, we need to prove that $\psi_k(x)$ is an eigenfunction of $\hat{T}$. Then, we prove that the translation operator $\hat{T}$ and the Hamiltonian $\hat{H}$ commute. So, Bloch's wavefunction is similarly an eigenfunction for the Hamiltonian with a periodic potential .

We need to find λ the eigenvalues of the translation operator $\hat{T}$:

$$\hat{T}\psi_k(x) = \lambda\psi_k(x) \tag{1.25}$$

If we apply $\hat{T}$on $\psi_k(x)$N times, and with periodic boundary conditions , one can find that :

$$\hat{T}^N\psi_k(x) = \psi_k(x + Na) = \psi_k(x) \tag{1.26}$$

From (1.22) , we can write :

$$\hat{T}^N \psi_k(x) = \lambda^N \psi_k(x) \qquad (1.27)$$

Which gives:

$$\lambda^N = 1 \rightarrow \lambda = e^{\frac{2\pi n}{N}} \qquad (1.28)$$

Where $= \pm 1, \pm 2 \ldots$.

Now, we can prove that $\psi_k(x)$ is an eigenfunction of the Hamiltonian by proving that $\hat{H}$and $\hat{T}$commute:

$$\hat{T}\hat{H}\psi_k(x) = \hat{T}[\frac{-\hbar^2}{2m_0}\nabla^2 + V(x)]\psi_k(x)$$

$$= [\frac{-\hbar^2}{2m_0}\frac{d^2}{d(x+a)^2} + V(x+a)]\psi_k(x+a)$$

$$= \left[\frac{-\hbar^2}{2m_0}\frac{d^2}{dx^2} + V(x)\right]\hat{T}\psi_k(x)$$

$$= \hat{H}\hat{T}\psi_k(x) \qquad (1.29)$$

So, the Hamiltonian commutes with the translation operator, which means that Bloch's function is an eigenfunction of the Hamiltonian stated in (1.20). We can write:

$$\psi_k(x+a) = U_k(x+a)e^{ik(x+a)} = e^{ika}U_k(x)e^{ikx} = e^{ika}\psi_k(x) \qquad (1.30)$$

In three dimensions:

$$\psi_k(r + T_n) = e^{ik.T_n}\psi_k(r) \qquad (1.31)$$

The eigenstates of the translation operator varies from one cell to another in the crystal with the phase factor e^{ikT_n}, The eigenstates of any periodic operator, such as the Hamiltonian, can be chosen with a definite values of k [3].

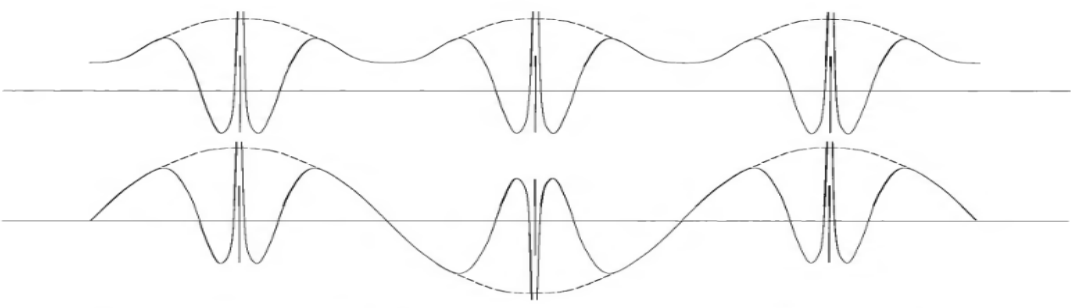

fig 1.6: schematic illustration of Bloch's function in one dimension

fig 1.6 shows a schematic illustration of Bloch's function in one dimension at k=0 and at the zone boundary k=π/a ,The envelope is the smooth function that multiplies a periodic array of atomic like 3S functions .

1.5. Conclusion

We have seen in this chapter the basic notions of crystalline structure and how the wavefunction of an electron behaves in crystal with a periodic potential. The most important notion that should be taken into consideration is the reciprocal space. We will see in further chapters that all the calculations will be done through the first brillouin zone, which is just the Wigner-Seitz cell of the reciprocal lattice. The EPM took advantage of the properties of the first brillouin zone.

Chapter 2: Empirical pseudopotential method

2.1. Introduction

Our band structures are computed using the empirical pseudopotential method with a model potential applicable to both the diamond and zincblende structures. As we know, the pseudopotential method exploit the fact that the electronic wave function may be separated into the sum of a rapidly oscillating part near the atomic cores and a slowly varying piece. The pseudopotential approach relies on the assumption that the core electrons are frozen and that the valence electrons move in a weak single electron potential making the true atomic wave function orthogonal to the core states.

2.2. Theoretical basis

Studies of electronic structure rely on knowledge of the energies and wavefunctions of single electron states throughout the Brillouin zone. To define the problem more clearly, we require the electronic structure to be known as a function of position in k-space:

$$E = E_n(k) \qquad (2.1)$$
$$\psi = \psi_n(k)$$

Where n is the band index, k is the wave vector, E is the energy, and ψ is the single electron wavefunction.

There are two general categories of methods to calculate the band structure [4]. The first category consists of ab initio methods, such as Hartree-Fock or Density Functional Theory (DFT), which calculate the electronic structure from first principles. In general, these methods utilize a variational approach to calculate the ground state energy of a many-body system, where the system is defined at the atomic level. The original calculations were performed on systems containing a few atoms. Today, calculations are performed using approximately 1000 atoms but are computationally expensive, sometimes requiring massively parallel computers . In contrast to ab initio approaches, the second category consists of empirical methods, such as the Orthogonalized Plane Wave (OPW)[5], tight-binding (also known as the Linear Combination of Atomic Orbitals (LCAO) method), and the local or the non-local empirical pseudopotential method (EPM). These methods involve empirical parameters to fit experimental data such as the band-to-band transitions at specific high-symmetry points derived from optical absorption experiments. The appeal of these methods is that the electronic structure can be calculated by solving a one-electron Schrödinger wave equation.

Thus, empirical methods are computationally less expensive than ab initio calculations and provide a relatively easy means of generating the electronic band structure [6].

In practice, the choice of which method to use is determined by the type of calculation that we are going to perform. For instance, it is obviously preferable to use a method which is reasonably fast in terms of CPU time if a large number of band structure calculations throughout the Brillouin zone are required which is exactly the case that we are dealing with. The empirical pseudopotential method perfectly serve our interest in this topic.

The empirical psodopotential method is a ground state theory with correspondingly empty conduction band states as a result; it does not give accurate conduction band energies. On the other side, ab initio methods does not give necessarily accurate results, and they are very CPU intensive. Fortunately, empirical methods are available that are less computationally expensive than ab initio calculations.

2.3. The empirical pseudopotential method

All band structure methods are required to solve the one-electron Schrodinger equation:

$$[\frac{-\hbar^2}{2m_0}\nabla^2 + V(r)]\psi(r) = E\psi(r) \qquad (2.2)$$

The difficulty in solving this lies in the potential term $V(r)$, which is the average potential felt by each electron and the ion cores. It has the periodicity of the crystal lattice and the property of being strong and atomic-like near the cores and weak between them. Several approaches such as Tight-binding method (TBM) and the nearly free electron model (NFEM) tend to solve that difficulty. But none of them achieves satisfactory. the TBM which is also known as LCAO (linear combination of atomic orbitals), gives acceptable valence band structure but can't be relied on for excited states, which are of obvious importance in any study of the optical properties. Also, the NFEM is an over-simplified model. this model consider the valence electron as a perturbed gas of a completely free electrons so that the potential in one electron Hamiltonian is considered to be smaller than the kinetic energy term , such that the energy can be expanded using perturbation theory. Fortunately, the pseudopotential method exists; it views the valence electrons as they are of primary importance in determining the properties of the crystal [7].

2.3.1 Element of the pseudopotetials

Electrons in atoms can be divided into two parts , core electrons and valence electrons .for example , the electronic configuration of Si is given by : $1s^2 2s^2 2p^6 3s^2 3p^2$,the $1s^2 2s^2$ and $2p^6$ considered as the core orbitals, and the $3s^2 3p^2$ forms the valence orbitals which are responsible for the bonding between atoms and can be modeled by the pseudowavefunction . The pseudowavefunction differs from the true wavefunction only in the ionic cores region that occupy a small fraction of the crystal volume, and obeys a Schrodinger-like equation with only a relatively weak potential. This assumption of a weak potential can be understood in terms of the fact that the valence electrons experience a nuclear potential that is screened by the core electrons and, in addition, the effect of the Phillips-Kleinman cancellation theorem[8]. The latter demonstrates that since the wavefunction of the valence electrons must be orthogonal to the core states, the pseudowavefunction behaves as if there is a repulsive "orthogonality potential". It turns out that the repulsive orthogonality potential and the attractive core potential almost cancel [9].

2.3.2. Orthogonalized plane waves (OPW)

in this section, a mathematical explanation for the arguments stated above is given . The basis states in this approach are constructed from a set of plane waves which have been orthogonalised to the atomic core states. Between the cores, the plane wave component is well suited to describe the weak potential that exists there. Near the cores, however, the orthogonalisation terms force the valence electron wavefunctions to adopt the next highest core state wavefunction, effectively acting to repel the valence electrons from the core. Thus these orthogonalisation terms act like a kind of repulsive potential, and when it is combined with the attractive core potential they almost cancel, leaving behind a net, weak effective potential. This is the pseudopotential. This effect is detailed in the Phillips-Kleinmann cancellation theorem [8], which explicitly demonstrates how such an orthogonality potential can be constructed. The true wavefunction is expressed as the sum of a smooth wavefunction ϕ and a sum over occupied core states ϕ_t:

$$\psi = \phi + \sum_t b_t \phi_t \qquad (2.3)$$

The true wavefunction is forced to be orthogonal the core states: $\langle \phi_t | \psi \rangle = 0$.

For all t, then solving for $b_t$yields:

$$\psi = \phi - \sum_t \langle \phi_t | \phi \rangle \phi_t \qquad (2.4)$$

Which can be substituted into the Schrodinger equation:

$$H\phi - \sum_t \langle \phi_t | \phi \rangle E_t \, \phi_t = E\phi - E \sum_t \langle \phi_t | \phi \rangle \phi_t \qquad (2.5)$$

This can then be rewritten in such a way as to explicitly identify the repulsive potential V_R arising from the orthogonalization terms:

$$(H + V_R)\phi = E\phi \qquad (2.6)$$

Where:

$$V_R = \sum_t (E - E_t)\phi_t \langle \phi_t | \phi \rangle / \phi \qquad (2.7)$$

If we then split up H into its kinetic component and core potential terms, we obtain:

$$\left(\frac{-\hbar^2}{2m_0}\nabla^2 + V + V_R\right)\phi = \left(\frac{-\hbar^2}{2m_0}\nabla^2 + V_{ps}\right)\phi = E\phi \qquad (2.8)$$

Where ϕ is a pseudowavefunction related with the true wavefunction by equation (2.3).

Equation (2.8) is the psudowavefunction ϕ equation. However, the energy term E does not represent a pseudoenergy. E is the true energy corresponding to the true wavefunction. As we can see in equation (2.8), the repulsive potential V_R and the attractive ionic cores potential V added to each other and almost cancel leaving a weak potential noted as pseudopotential.

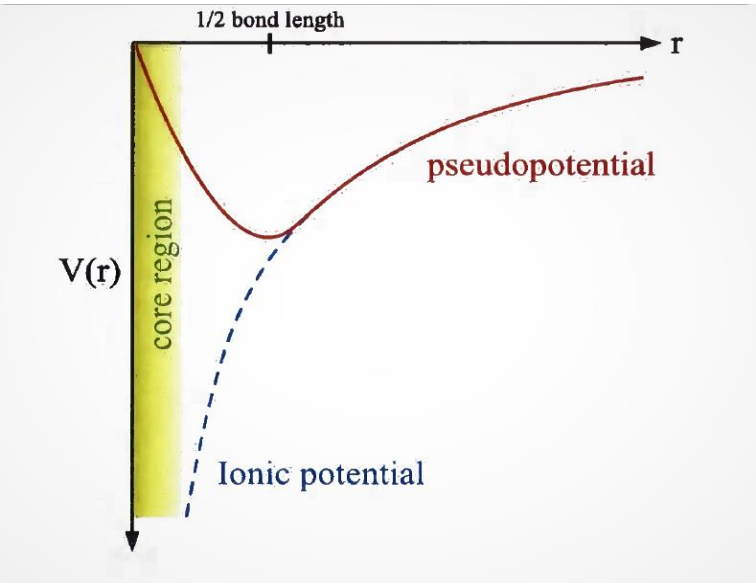

fig 2.1 : Schematic representation of the actual potential and its correspondent pseudopotential.

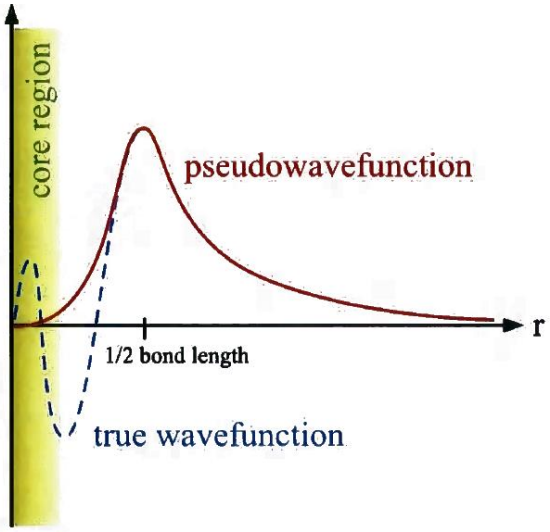

fig 2.2 :Schematic representation of the actual wavefunction

and corresponding Pseudowavefunction

fig 2.1 is a representation of the true potential and its corresponding pseudopotential. ***Fig 2.2*** represents the true and the pseudowavefunction. Near the nucleus, the ionic potential diverges, but the pseudopotential weakens, as a result the true wavefunction for the ionic potential has rapid spatial oscillations near the core, but the pseudowavefunctionis quite smooth. Both the potential and pseudopotential, and the wavefunction and pseudowavefunction become identical far away from the core. Although the true wavefunction and pseudo-wavefunction differ near the ionic cores, the ionic cores only constitute a small fraction of the crystal volume.

The previous explanations ensure the advantage of the pseudopotential method in term of CPU times. If we described the true wave function of the crystal using plane wave, a large number of plane waves would be needed to make the calculations more accurate. This is because of the strong oscillations of the true wavefunction near the core region. With such a large number of plane waves, calculations will be so CPU intensive and would take a long time. However, when we use the pseudopotential approach, a much smaller number of plane waves would be required to get acceptable results. That what makes the EPM a powerful tool, because it provide a good approximation in less CPU times than ab initio approximations.

2.3.3. Solution of the pseudo-Hamiltonian

Energies and psudowavefunctions are obtained by solving equation (2.8)[7]. which can be written this way:

$$(\frac{-\hbar^2}{2m_0}\nabla^2 + V_{ps})\psi = E\psi \qquad (2.9)$$

Where $V_{ps}$is the smoothly varying crystal pseudopotential. It has to process the periodicity of the lattice , we can write then :

$$V_{ps}(r) = V_{ps}(r + T_n) \qquad (2.10)$$

Where T_n is a vector in the real space. In general, V_{PS} is the smoothly varying crystal pseudopotential. In general, V_{PS} is a linear combination of atomic potentials V_a, which can be expressed as summation over lattice translation vectors R and atomic basis vectors τ to arrive at the following expression:

$$V_{ps}(r) = \sum_R \sum_\tau V_a(\mathrm{r} - \mathrm{R} - \tau) \qquad (2.11)$$

To simplify further, the inner summation over τ can be expressed as the total potential, V_0, in the unit cell located at **R**. equation (2.11) then becomes:

$$V_{ps}(r) = \sum_\mathrm{R} V_0(\mathrm{r} - \mathrm{R}) \qquad (2.12)$$

We know that $V_{ps}(r)$ is a periodic function, this means that V_{ps}can be written in a Fourier representation:

$$V_{ps}(r) = \sum_m V_0(G_m)\, e^{iG_m.r} \qquad (2.13)$$

G_m is a vector in the reciprocal space. This a local pseudopotential where there is no dependence on the angular momentum.

the expansion coefficient $V_0(G_m)$ is given by:

$$V_0(G) = \frac{1}{\Omega}\int_\Omega V_0(r)e^{-iG.r}\, dr \qquad (2.14)$$

Ω is the primitive unit cell volume. $V(G)$ also referred to us as the pseudopotential form factor.To apply this formalism to the zincblende lattice, it is convenient to choose a two-atom basis centered at the origin (R = 0). The atomic basis vector for the zincblende structure are given in equation (1.7), $V_0(r)$ can be expressed as:

$$V_0(r) = V_1(r-\tau) + V_2(r+\tau) \qquad (2.15)$$

WhereV_1, V_2 are the atomic potential of the cation and the anion.

Substituting equation (2.15) into equation (2.14) and using the displacement property of Fourier transforms, V_0(r) can be recast as :

$$V_0(G) = V_1(\mathrm{G})e^{i\mathrm{G}\tau} + V_2(\mathrm{G})e^{-i\mathrm{G}\tau} \qquad (2.16)$$

Writing the Fourier coefficients of the atomic potentials in terms of symmetric($V_s = V_1 + V_2$) and antisymmetric($V_A = V_1 - V_2$) form factors , $V_0(G)$ can have these form :

$$V_0(G) = \cos(\mathrm{G}.\tau)V_s(G) + i\sin(\mathrm{G}.\tau)V_A(G) \qquad (2.17)$$

Where the prefactors are the symmetric and antisymmetric structure factors. The form factors above are treated as adjustable parameters that can be fit to experimental data.

For diamond-lattice materials, with two identical atoms per unit cell, the V_A=0 and the structure factor is simply $\cos(\mathrm{G}.\tau)$. For zincblende lattice, like the one in GaAs material system, V_A≠0 and the structure factor is more complicated [6].

Now, Bloch's theorem can be employed to rewrite the wave function $\psi_k(r)$:

$$\psi_k(r) = e^{ik.r}u_k(r) \qquad (2.18)$$

Where $u_k(r)$ has the periodicity of the crystal lattice. It can be expressed using Fourier sum employing N plane waves :

$$u_k(r) = \sum_{n=1}^{N} a_n(k)e^{iG_n.r} \qquad (2.19)$$

If we put the potential in equation (2.11) and the wavefunction in equation (2.18) into schrodinger equation (2.9) , the problem is reduced to a standard matrix eigenvalue problem :

$$\begin{pmatrix} A(1) & V_{PS}(1,2) & \cdots & V_{PS}(1,N) \\ V_{PS}(2,1) & A(2) & \cdots & V_{PS}(2,N) \\ \vdots & \vdots & \ddots & \vdots \\ V_{PS}(N,1) & V_{PS}(N,2) & \cdots & A(N) \end{pmatrix} \begin{pmatrix} a_1 \\ a_2 \\ \vdots \\ a_n \end{pmatrix} = E \begin{pmatrix} a_1 \\ a_2 \\ \vdots \\ a_n \end{pmatrix} \qquad (2.20)$$

where the individual matrix elements are given by :

$$A(i) = \frac{\hbar^2}{2m_0}(K + G_i)^2 + \langle K_i|V_{ps}(r)|K_i\rangle$$
$$V_{ps}(i,j) = \langle K_i|V_{ps}(r)|K_j\rangle \quad (2.21)$$
$$K_n = e^{i(k+G_n).r}$$

The solution of this precedes using standard matrix diagonalization routines. If N plane waves are used in the expansion at a given k, N eigenvalues are obtained corresponding to the energies of the bands at that k. Each of these eigenvalues also has an associated eigenvector whose coefficients (a_1,a_2,…,a_n) describe the wavefunction of that band at k. Hence diagonalization of the matrix results in N eigenvalues and N eigenvectors. It is instructive to restate the advantage of the pseudopotential approach in quantitative terms at this point. If the real potential was used in Equation (2.20) then the rapid oscillations of the wavefunctions in the core would require an expansion involving of the order of 10^6 plane waves, corresponding to a $10^6 \times 10^6$matrix. This makes the problem nearly very hard to solve, since the number of calculations required to solve the Hamiltonian is proportional to N^3, where N is the order of the matrix. Use of the pseudopotential reduces this problem to a manageable one, with the order of 50 plane waves per atom in the unit cell usually being sufficient to obtain a reasonably well converged representation [7].

2.3.4. Choice of the pseudopotential

There are two main choices for the exact form of the pseudopotential, the local and the non-local pseudopotential. It was shown previously using the Phillips-Kleinmann theorem how the pseudopotential can be constructed by knowing only the core states. However, although this theorem does serve to underline why the pseudopotential method works, practically, other technics are used to obtain pseudo potentials. For most such approaches, a parameterized model for the potential is chosen, the final form of which is obtained by fitting to known data from experiment.

Cohen and Bergstresser [10], chose to adopt a simple local form of the pseudopotential where the angular momentum is not taken into consideration. This technique was successfully used for Germanium and Silicon before being extended to other common semiconductors. However, after consideration of the Phillips-Kleinmann formulation of the pseudopotential, it is obvious that it must possess some nonlocal character. This is because the pseudopotential is constructed from a summation over the core states, and can thus be split up into its constituent V_S , V_P , V_d etc contributions. It becomes clear that if the core does not contain electrons of a certain angular momentum then there will be no repulsive potential for that component.

Carbon, for example, has a core which is$1s^2$, and thus the *p*-valence electrons will feel no repulsive potential. It should be noted that in practice, however, the precise form of the local potential might be chosen to give correct results for a given symmetry state. Therefore, even if there are no *p* or *d* core states it does not necessarily mean that there are no *p* or *d* components [7].

We should note that in addition to the local and the non-local pseudopotential, spin orbit coupling effects must be included too. Leaving a final form for the matrix elements of the pseudopotentialas:

$$\langle k_i|V_{ps}|k_j\rangle = \langle k_i|V_l + V_{nl} + V_{so}|K_j\rangle \qquad (2.22)$$

Where V_l pseudopotential, $V_{nl}$is the non-local pseudopotential, V_{so} is the contribution due to spin-orbit coupling. All these elements are discussed in the next sections.

2.3.5. The local pseudopotential

The form of the pseudopotential for one atom per primitive unit cell is:

$$V_l(r) = \sum_m V(G_m)\, e^{iG_m.r} \qquad (2.23)$$

The pseudopotential form factor $V(G_m)$ is given by:

$$V(G) = \frac{1}{\Omega}\int_\Omega V(r)e^{-iG.r}\, dr \qquad (2.24)$$

Where Ω is volume of the primitive unit cell. Different number of form factors can be employed for different structures.

2.3.6. The non-local pseudopotential

We stated earlier that the pseudopotential should possess some non-local character, even though in actual calculations these contributions are often ignored. Including non-local character would make calculations more accurate. The nonlocal pseudopotential is incorporated by placing spherical potential wells around each ion, each of which act on a different angular momentum component of the wavefunction. The matrix element contribution from the nonlocal pseudopotential is written in the form [7]:

$$\langle K_i|V_{nl}|K_j\rangle = \sum_l \langle k_i|A_l(E)\mathrm{f}_l(r)\hat{P}_l|K_j\rangle \qquad (2.25)$$

Where $A_l(E)$is the well depth, $\mathrm{f}_l(r)$describes the shape of the well, and $\hat{P}_l$ is a projection operator such that the *lth* well acts only upon the *lth* angular component of the wavefunction.

The summation is over the angular momentum components l present in the core wavefunctions.

The well depth $A_l(E)$is in general a function of energy. It is usually sufficient to adopt a fixed depth A_2 for the *d* well, but a more complicated form is used for the *s* well depth. The inclusion of a nonlocal component in the pseudopotential introduces a total of up to 5 new parameters per atomic type, some of which such as the interatomic separation are fixed.

2.3.7. spin orbit coupling

Spin-orbit coupling is the interaction of the electron spin and its orbital angular momentum which causes the degeneracy of some of the electron states in the crystal to be lifted. It is a relativistic phenomenon and is therefore more pronounced in the heavier elements [7]. The electronic states of nitrogen are known to dominate the electronic structure at the top of the valence band, where the effect of spin-orbit coupling is expected to be most noticeable. Although nitrogen is a light element, the spin-orbit splitting cannot be ignored without undue error. The matrix elements due to the spin-orbit interaction is written as:

$$\langle K_i|V_{S0}|K_j\rangle = (K_i \times K_j).\sigma_{s,s}[-i\lambda^s.S^s(G_i - G_j) + \lambda^A.S^A(G_i - G_j)] \qquad (2.26)$$

Where

$$K_i = k + G_i \qquad (2.27)$$

$$K_j = k + G_j$$

$$\lambda^s = (\lambda_c + \lambda_a)$$

$$\lambda^A = (\lambda_c - \lambda_a)$$

$$\lambda_c = \mu B^c_{nl}(K_i)B^c_{nl}(K_j)$$

$$\lambda_c = \alpha\mu B^a_{nl}(K_i)B^a_{nl}(K_j)$$

$$B_{nl}(K) \propto \int_o^\infty jnl(K_r)R_{nl}(r)r^2dr$$

Where $jnl(K_r)$ is the spherical Bessel function of the lth angular momentum component and $R_{nl}(r)$is the radial part of the core wavefunction. The matrix element contributions due to the anion and cation are more simply written as:

$$\langle K_i|V^a_{so}|K_j\rangle = -\mu i\langle v_i|\sigma|v_j\rangle.(K_i \times K_j) \qquad (2.28)$$

$$\langle K_i|V_{so}^{\beta}|K_j\rangle = -\alpha\mu i\langle v_i|\sigma|v_j\rangle.(K_i \times K_j)$$

Spin-orbit coupling has been incorporated into the pseudopotential scheme by wiez [11], and others [12] [13]. As stated above, spin orbit coupling have greater effect in heavier materials. Therefore, there is no difference between this approach and the approach adopted by Bloom and Bergstresser for the materials considered in this thesis. The parameter μ is an adjustable parameter, altered so as to reproduce the required valence band splitting. The immediate effect of including the spin-orbit coupling in the calculations is a doubling in the size of the matrices involved. When including spin, the size of the matrices becomes 2N×2N increasing computational load. Chelikowsky and Cohen [14] deals with this doubling by treating spin orbit interactions as a perturbation.

2.4. Fitting of the pseudopotentials

Experimental information is incorporated into the pseudopotentials through the symmetric and antisymmetric pseudopotential form factors. Band structure information for a particular material is obtained from experiment or from more fundamental calculations. This band structure data is used to determine a set of $V_S(G)$and $V_A(G)$ that define the pseudopotential for the specific reciprocal lattice vectors of the material in question. The simplest approach is to fit the set of $V_S(G)$ and$V_A(G)$ directly to the band structure data. Data for form factors established in this way are available in the literature (for example [15]). This approach is well established and has proved to be a very successful tool in the calculation of electronic structure [16][17], but there is no ready way to use the results to obtain the form factors of the material when strained, or of alloys made from the material. An alternative approach, which is used throughout this topic, is to parameterize the functions $V_S(q)$and $V_A(q)$for a range of continuous q values, such that the form factors could be obtained for any reciprocal lattice in that range. This approach provides more flexibility, as the reciprocal lattice vectors can be varied as the lattice constant changes with strain or alloying [9]. The symmetric and antisymmetric functional forms of the pseudopotentials can be given by [18][19]:

$$V_S = \frac{a_1 q^2 + a_2}{1+\exp(a_3[a_4 - q^2])} \qquad (2.29)$$

$$V_A = (a_1 q^2 + a_2)\exp(a_3[a_4 - q^2]) \qquad (2.30)$$

Where a_i , i= 1 to 4 , are the parameters to be adjusted in the fitting procedure. q is in units of $(2\pi/a_{zb})$,where $a_{zb}$is the lattice constant of the zincblende form of the relevant material. The

respective form factors V(G), at the particular G values required in the band structure calculations, can then be simply obtained from these expressions .

The empirical pseudopotential parameters are optimized using the non-linear least-squares method, which requires that the root-mean-square deviation of the calculated level spacing (LS) from the experimental ones defined by:

$$\delta = \left[\frac{\sum_{(i,j)}^{m}\{\Delta E^{(i,j)}\}^2}{(m-N)}\right]^{\frac{1}{2}} \quad (2.31)$$

Should be minimum [7].

2.5. Output of the EPM

After obtaining the necessary parameters for the local and the non-local pseudopotential, and the spin-orbit interactions, the solution of the matrix constituted of 2N×2N can be done using standard matrix diagonalization methods, giving as a result, the energies and the pseudowavefunction:

$$E_n(k), n = 1, \cdots, 2N \quad (2.32)$$

$$C_n(k), n = 1, \cdots, 2N \quad (2.33)$$

Where n is the band index. The pseudowavefunctions are generally a complex vector quantities:

$$C_n(k) = [\uparrow C_{n,1}(K), \cdots, \uparrow C_{n,N}(K), \downarrow C_{n,1}(K), \cdots, \downarrow C_{n,N}(K)] \quad (2.34)$$

As a result, the pseudowavefunction have the following form:

$$\psi_n(k) = u_n(k)e^{ik.r} = \frac{1}{\Omega}\left[\sum_{j=1}^{N}(\uparrow c_{n,j}|\uparrow\rangle + \downarrow C_{n.j}|\downarrow\rangle)e^{iG_j.r}\right]e^{ik.r} \quad (2.35)$$

Where $u_n(k)$ is the Bloch periodic part of $\psi_n(k)$and Ω is the unit cell volume. The eigenfunctions $|\uparrow\rangle$ and $|\downarrow\rangle$ denote spin-up and spin-down states respectively.

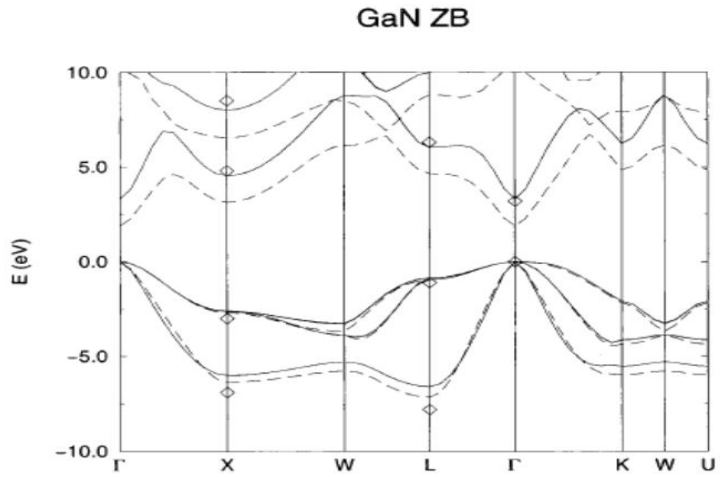

fig 2.3 : example of a zincblende band structures GaN.

The ***fig 2.3*** shows the deference between a band structures for zincblende structure calculated using the first principals code VASP (dashed lines), and when using the empirical pseudo potential method (solid lines).

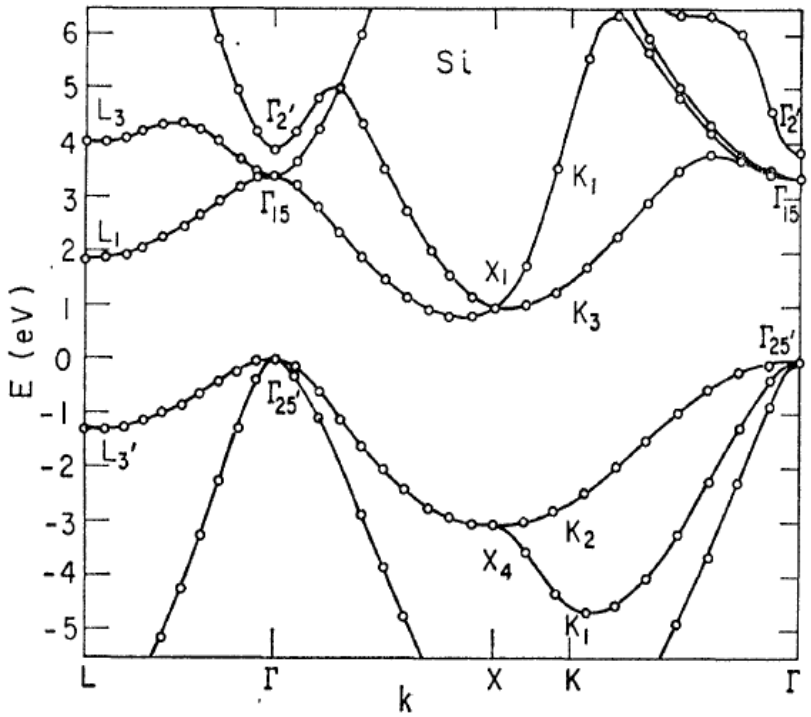

fig 2.4 : band structures for a diamond structure material (Si)

fig 2.4 shows the band structure of silicon calculated by Cohen an Bergstresser [10], using the empirical pseudopotential method.

2.6. Conclusion

The EPM was introduced briefly in this chapter. All the necessary elements for our calculations of band structures have been highlighted and explained. We are going to use this method in order to calculate the band structure for two structures: Diamond and Zincblende in the next chapter. It is important to note that the EPM is the most convenient choice for such application due to the accurate results that it gives when compared to the time that it take.

Chapter 3: Implementation, results, and discussion

3.1. Introduction

The previous two chapters were devoted to the presentation of details around semiconductors structures and theoretical models that could help describing features of those semiconductors. Much attention was given to the pseudopotential approach since this is the model we will implement numerically to present results that show the efficiency of such an approach. For this, we will use Fortran language to encode the established algorithm. For the diagonalization issue we will use the LAPACK (linear algebra package) libraries since this will make the encoding more tractable. Therefore, it is necessary to review Fortran programming language and highlight its various benefits. Then, introduce LAPACK libraries, and how the diagonalistion process become very easy when using these libraries. After that, the details of the program are given. As a final part of this project, we are going to apply this model to both diamond and zincblende structure and discuss the different results.

3.2. Technical details

3.2.1. Fortran programing language

Fortran is a general-purpose programming language; its name is derived from the sentence FORmula TRANslation. This language first developed in 1957 at the famous company IBM, and then the American standards association released the first version of Fortran in 1966, named Fortran 66. The purpose of developing Fortran was to provide a portable standard language which can be easily transferred from a computer to another. Since the start of fortran development , there have been many version and releases of fortran, a revised version of Fortran 66 was released in 1977 and named Fortran 77 . Then, a better version when compared to Fortran 77 was released in 1990; it contains a lot of features beside the Fortran 77 features. Followed by a 1995, 2003, 2008, 2018 versions. Every new version introduces new features and fixes issues of last version.

Fortran was the first high level programming language and the most preferred language for the scientist over time, Due to its availability and simplicity which make it easy to teach and learn.

Fortran is rarely used in industry today, and there are many competing languages that gives many features in a better way than Fortran do (ex: C++, python, matlab …). in term of speed , C++ is a bit faster than Fortran , and in term of simplicity , python is easier to learn than any other languages , but it's not the best choice for heavy numerical computation, because it is very slow when compared to C++ and Fortran . This leaves us with two choices, either you chose the more updated and the faster language that is C++, or chose Fortran. The most important feature supplemented by Fortran is maybe the fact that is highly oriented object and then is very close to the machine. This can have a great advantage over memory allocation and management. Besides most of physics code legacy is written in Fortran and it is much easier to accommodate with this than write a new piece of programming. A very true example of this is the LAPACK libraries that are a valuable piece of programs written in Fortran and that are very useful for encoding.

3.2.2. Diagonalization with LAPACK libraries

Diagonalization is the process of finding the eigenvalues and the eigenstates for a dagonalizable matrix. A matrix "A" is diagonalizable when there exist a diagonal matrix and an invertible matrix P such that $A = PDP^{-1}$. When D and P are found for a given A, we say that A has been diagonalized . if $A_{n\times n}$ is diagonalizabe, then A has n linearly independent eigenvectors. Also in the equation $= PDP^{-1}$, P is a matrix whose columns are eigenvectors $\overrightarrow{a_i}$, and the diagonal entities of D are eigenvalues λ_i corresponding column by column to their respective eigenvetors. the eigenvalue problem can be written in the following form : $D\overrightarrow{a_i} = \lambda_i\overrightarrow{a_i}$.

Since matrices are the beating heart of physics, Diagonalization then would be also very important, especially in quantum physics. The basic reason of this application is that the time-independent Schrödinger equation is an eigenvalue problem. For our project, we are going to elaborate diagonalization of the secular equation from chapter two using linear algebra package (LAPACK) for Fortran. so what is LAPACK and what is the advantage of using it ?

the LAPACK (Linear Algebra Package) is written in Fortran 90 and provides routines for solving systems of simultaneous linear equations, least-squares solutions of linear systems of equations, eigenvalue problems, and singular value problems. The associated matrix factorizations (LU, Cholesky, QR, SVD, Schur, generalized Schur) are also provided, as are related computations such as reordering of the Schur factorizations and estimating condition

numbers. Dense and banded matrices are handled, but not general sparse matrices [20] . In all areas, similar functionality is provided for real and complex matrices, in both single and double precision. LAPACK routines are written so that as much as possible of the computation is performed by calls to the Basic Linear Algebra Subprograms (BLAS). LAPACK is designed at the outset to exploit the Level 3 BLAS, a set of specifications for Fortran subprograms that do various types of matrix multiplication and the solution of triangular systems with multiple right-hand sides.

In Fortran programs, most LAPACK routines can be invoked with the CALL statement, such as CALL Routine-name (argument_1, ..., argument_n). The following is an example:

CALL DGETRF(m, n, A, lda, ipiv, info); "DGETRF is an example of a LAPACK routine"

3.3. Implementation strategy

3.3.1. Summary of the formulations

As we have explained in the second chapter the central issue in the theoretical quantal study is the resolution of the Schrodinger equation. In fact this will lead to the eigenfunctions and eigenvalues that are sufficient to deduce any feature related to our semiconductor structure. As we have showed the difficulty reside in the fact that the potential to use in this equation is quite ubiquitous and to overcome this obstacle the use of the pseudopotentiel could be very helpful and less cumbersome compared to others approaches.

The final set of equations we terminated with at the end of the development of pseudopotential technique were:

$$\begin{pmatrix} A(1) & V_{PS}(1,2) & \cdots & V_{PS}(1,N) \\ V_{PS}(2,1) & A(2) & \cdots & V_{PS}(2,N) \\ \vdots & \vdots & \ddots & \vdots \\ V_{PS}(N,1) & V_{PS}(N,2) & \cdots & A(N) \end{pmatrix} \begin{pmatrix} a_1 \\ a_2 \\ \vdots \\ a_n \end{pmatrix} = E \begin{pmatrix} a_1 \\ a_2 \\ \vdots \\ a_n \end{pmatrix} \qquad (3.1)$$

Where :

$$A(i) = \frac{\hbar^2}{2m_0}(K + G_i)^2 + \langle K_i | V_{ps}(r) | K_i \rangle$$

$$V_{ps}(i,j) = \langle K_i | V_{ps}(r) | K_j \rangle \qquad (3.2)$$

$$K_n = e^{i(k+G_n).r}$$

It can be stated straightforwardly that the problem resolves by using any diagonalization technique to find the a_i and E. However as we have showed before the choice of pseudopotential V_{ps} imposes some constraints. For our study we will just consider the non-local case with the value of the structural factors given by the experimental measures [21]. The contribution of these structural factors is limited to only three factors (as the higher orders vanishes to very negligible values)

3.3.2. Number of the plane waves and the cutoff energy

The summation for the Fourier transform that define the potential as well as the wave function is in infinite by definition. To implement this in a program it is mandatory to cut the basis at a certain value to make the calculations feasible. The only way to establish the limit is to identify the value of the energy at which the calculations seem to converge towards a stable value. It is what we call cutoff energy that the user should test for each studied case. The value of the cutoff energy determine in turn the number of the plane waves needed in our basis. As showed before, the pseudopotential allows the cancellation of the core contribution which is highly localized and varying very rapidly making the number of the waves needed to describe the variations enormous. The cancellation of the core contribution renders the solution numerically reachable.

For our program we need an estimation of the maximal index that can be used as a number of plane wave. For this we use the following estimation:

$$n_{max} = \frac{\sqrt{E_{cut}}}{2\sqrt{3}\frac{\pi}{a}+0.5} + 1 \qquad (3.3)$$

Where a is the lattice parameter.

3.3.3. Symmetric and antisymmetric contributions to the potentials

Cohen and Bergstresser introduce a "symmetric" and an "antisymmetric" contribution, corresponding respectively to a cosine and a sine times the imaginary unit in the structure factor. The potential elements is given by the following equation:

$$< b_{i,k} |V| b_{i,k} > = Vs(G)\cos(G \cdot d) + iVa(G)\sin(G \cdot d) \qquad (3.4)$$

Where

$$b_{i,k} = k + G_i \qquad (3.5)$$

This illustrate the real and the complex parts of the potential where i is the imaginary unit and the d is the interatomic distance.

We intend to test first our programm for diamond-lattice as for silicon (Si), Germanium (Ge) and tin (Sn). For those cases the atoms are identical and the antisymmetric contribution to potential is zero, and we end up with real value of all the matrix compounds for the systems of equation (3.1). The diagonalization in this case is easily performed using routine like Dysev from Lapack.

For the zincblende (like GaP, GaAs…) however the cell contains two different type of atoms and the potential are complex number. We faced problems of numerical stability using directly diagonalization routines dealing with double precision complex. To avoid this problem by exploiting the fact that our complex matrix are still hermitian, we transform them to real matrices by using the routine "chetd2". This will convert the problem to the same process as previously.

3.3.4. Bands structure calculation

For each value of the wave vector k, a set of eigenvalues is deduced by resolving the secular equation. The connection between this energies form the bands structure. The values of k are introduced as an input for the program and could be selected along any chosen high symmetry points. Four our program we output four valence bands and four conduction bands. The bands structure is important to determine whether the semiconductor gap is direct ou indirect : if the maximum of the last valence band and the minimum of the first conduction band coincide at the point Gamma, then the semiconductor is said to posse a direct gap and its gap is indirect otherwise. The Fermi level is the energy separating the last valance band and the first conduction band.

3.3.5. Charge density

The eigenvectors that are the output of the resolution of the secular equation could be used to plot the charge distribution. In Fact this will lead to the construction of the wave function which the modulus will give the probability density that is directly connected to the charge distribution. It can be highly instructive to look to those distributions as it can give valuable

information on the nature of the bonds between atoms whether for example it is covalent or rather ionic.

3.3.6. Architecture of the program

In the following we give a very compact representation of the written program:

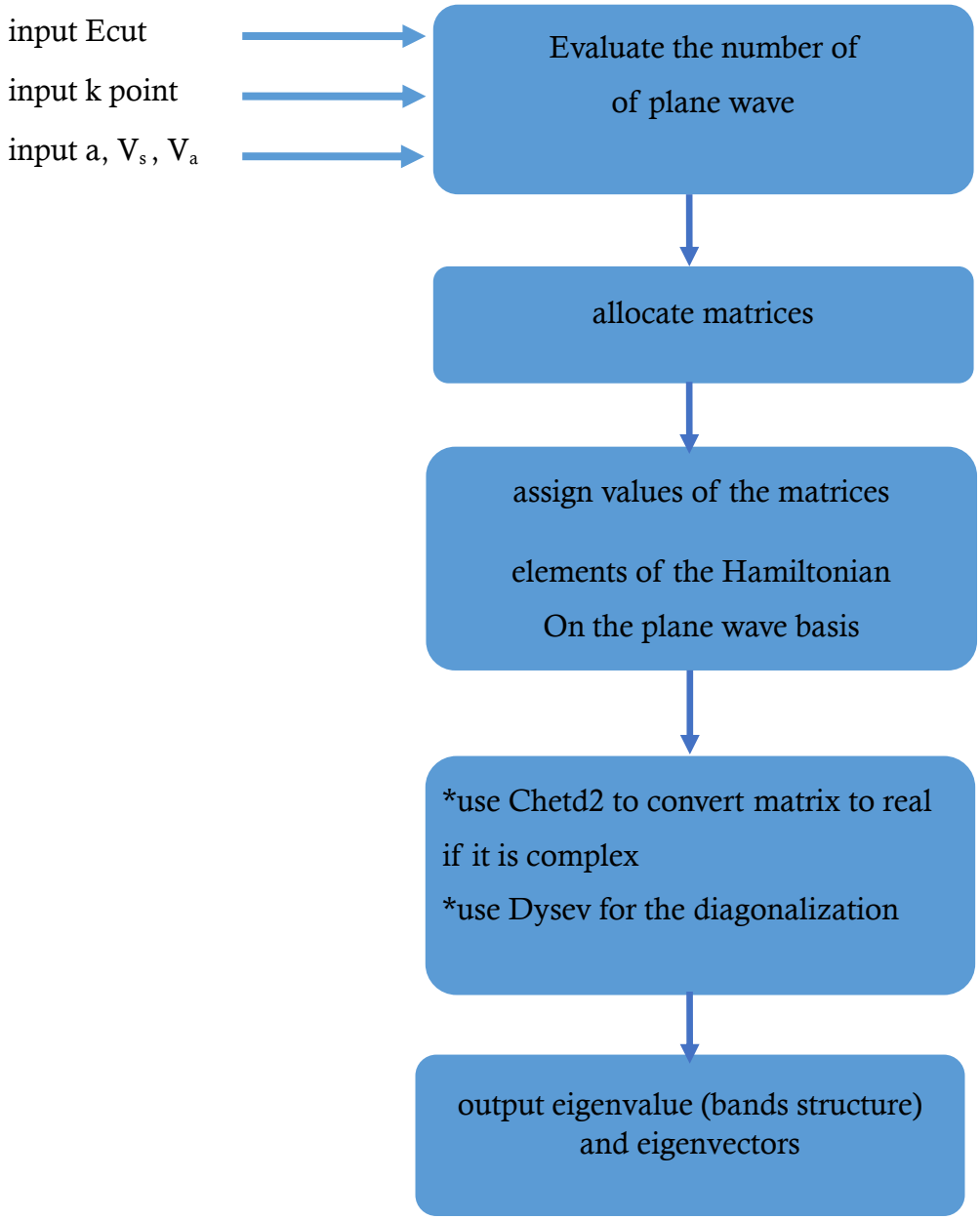

***fig 3.1*:** Representation of the architecture of the built program

It is important to notice here that the matrices are allocate dynamically according to the plane wave number determined by the input phase.

3.4. Results and evaluation

After have presenting the most important data about our program we are going to test the performance of the established program on some specific examples. For the diamond structure we will check the results for Si, Ge and Sn whereas for the zincblende structure we are going to illustrate the results for GaP, GaAs, and AlSb. Table 3.1 summarize the value of the most important input for the program [21]. The cutoff energy is found to turn around 10 Rydberg for all the cases. The k points are chosen along L (k modulus =0.866), Γ (k modulus=1.73), x (k modulus=2.82), Γ. All the plots of the band structure are versus the k modulus.

	Lattice Constant (A)	V_3^S	V_8^S	V_{11}^S	V_3^A	V_4^A	V_8^A
Si	5.43	-0.21	0.04	0.08	0	0	0
Ge	5.66	-0.23	0.01	0.06	0	0	0
Sn	6.49	-0.2	0	0.04	0	0	0
GaP	5.44	-0.22	0.03	0.07	0.12	0.07	0.02
GaAs	5.64	-0.23	0.01	0.06	0.07	0.05	0.01
AlSb	6.13	-0.21	0.02	0.06	0.06	0.04	0.02

***Table3.1*:** Values of the data used as input for the studied cases [21]

3.4.1. Diamond structure

3.4.1.1. Silicon (Si)

The bands structure is illustrated in ***fig 3.2***. The details of the bands could vary slightly according to the points chosen for the plot but we can notice that the major features are well reproduced by our calculations. For the comparison the reader can refer to the original paper of Cohen and Bergstresser [10] or any representation on the web. We can notice also that the gap for Silicon is indirect as expected. The value of the energy at the gamma point reproduced by our calculation is 3.4 eV in excellent accordance with the experimental value. The value of the gap is 0.9 eV.

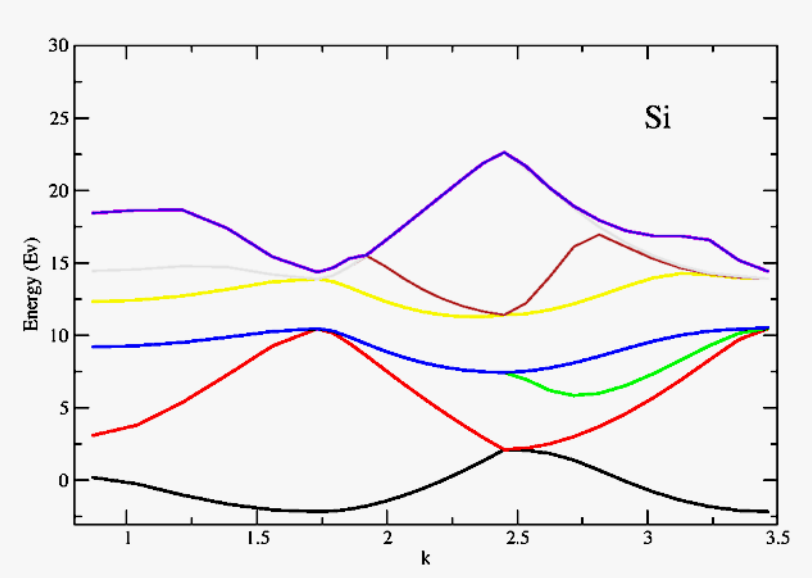

fig.3.2: Silicon bands structure

3.4.1.2. Germanium (Ge)

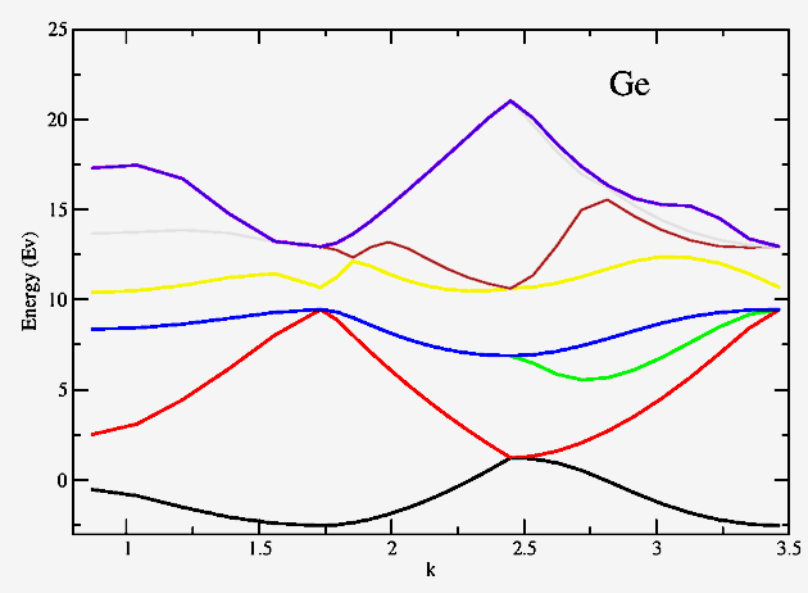

fig.3.3: Germanium bands structure

fig.3.3 illustrates the band structure for Germanium. The gap is direct with the value given by our calculation of 1.2 eV.

3.4.1.3. Tin (Sn)

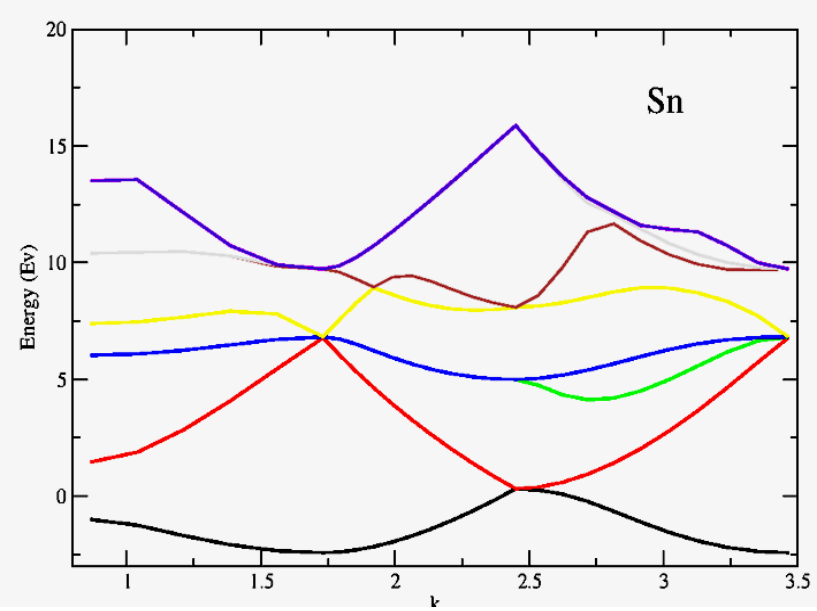

fig.3.5: Tin bands structure

fig 3.5 illustrates the band structure of Sn. The gap is direct with the value of our calculation around zero.

3.4.2. Zincblende structure

3.4.2.1. Gallium phosphide (GaP)

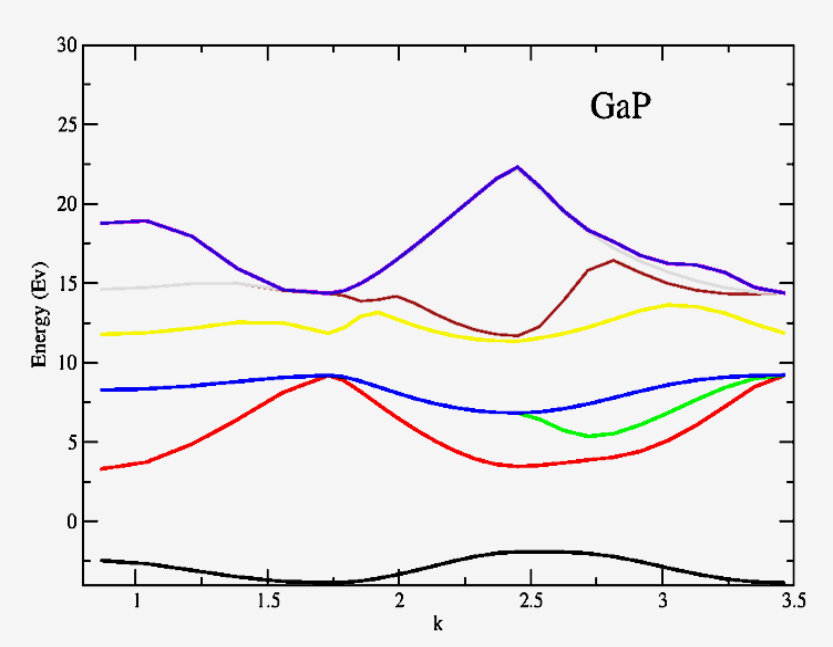

fig.3.5: GaP bands structure

fig.3.5 illustrates the band structure for GaP. The gap is direct with a value of 2.76 eV

3.4.2.2. Gallium arsenide (GaAs)

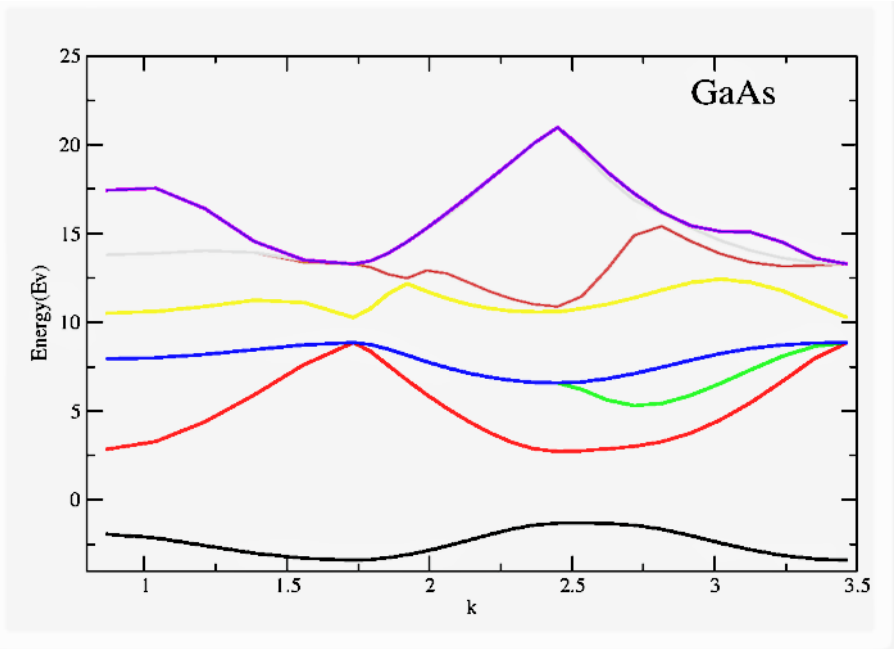

fig.3.6: GaAs bands structure

fig.3.6 illustrates the band structure for gaAs. The gap is direct with a value of 2.64eV given by our calculations.

3.4.2. 3. Aluminum antimonide (AlSb)

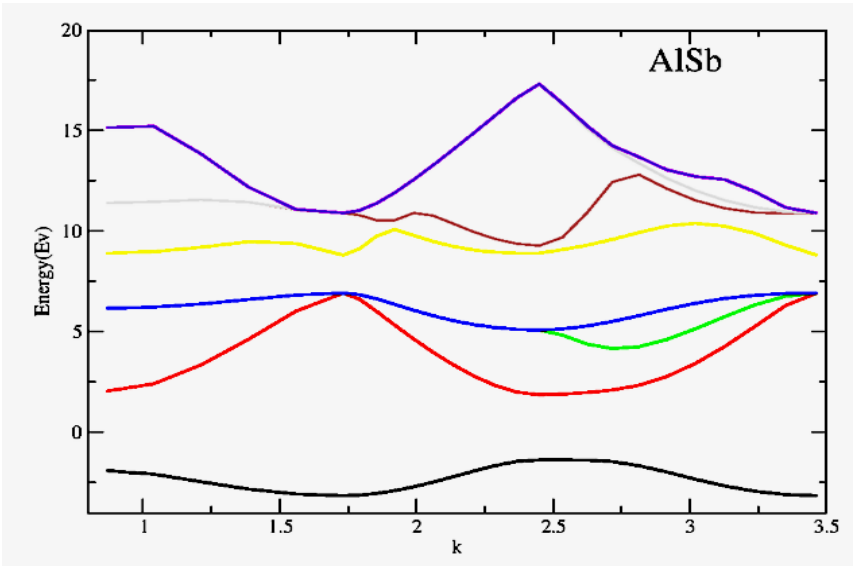

fig.3.7. AlSb Bands structure

fig.3.7 illustrates the band structure for AlSb. The gap is direct with a value reproduced by our calculations of 1.89 eV.

	Type	Calculated gap (eV)	experimental gap (eV) *
Si	indirect	0.9	1.11
Ge	direct	1.2	0.74
Sn	direct	0	0
GaP	direct	2.76	2.32
GaAs	direct	2.64	1.42
AlSb	direct	1.89	1.58

* measures from https://www.mtixtl.com/bandgap-semiconductor.aspx

Table 3.2*:* Comparison of the calculated gap to the measured value [22]

We compare in table 3.2 the calculated gap energies to those reported in the literature. The comparison is quite satisfactory especially when bearing mind the simplicity and rapidity of the used approach. As the gap is temperature dependent, the comparison holds only for 300 K.

3.5. Conclusion

In this study, we used empirical pseudopotentials to find the band structures for 6 diamond and zincblende crystals. The time-independent Schrödinger equation was expanded in plane waves of the reciprocal lattice. The eigenvalues of the resulting Hamiltonian matrix were found using computational methods, and the band structures were plotted. The found results for the gap energy compare well with experimental data.

Conclusion

Using computer simulation to determine physical features for materials has become a non avoidable tool to do physics nowadays. Henceforth multiple codes ready-to-use are available on the market each with its benefits, limitations of use and problems. It is however very important to be aware of the details of the "black box" if we want to be critical not only about the simulation results but also about the process that has lead to such a result. Consequently it is very important to do computational physics to investigate different possibilities at the level of modelization and numerical recipes.

The project of this study was the investigation of the empirical pseudopotential method and its contribution in the characterization of some semiconductors. The final goal was to be able to write a program that is simple and can give results in less time.

We have started our investigation by presenting the philosophy of the pseudopotential method which can be summarized in one fact: cancel the contribution of the core making the needed basis small enough for a practical calculations. Expanding this way the Schrodinger equation on the plane wave basis using the Fourier transform lead us to the secular equation which is the starting point for the numerical treatment.

The written program uses Fortran for encoding the algorithm and the Lapack libraries for the diagonalization routines. Solutions were to be found to avoid numerical instabilities by exploiting the hermitian nature of the matrices used in these calculations.

Once the software is built, we performed calculations on some specific semiconductors to show the efficiency of the established tool. The band structure for six diamond and zincblende semiconductors were investigated and presented. The comparison with plots that could be found in the literature is quite satisfactory. To quantify more the agreement, we compared the calculated gap energy with measured values. Here also the agreement is quite satisfactory.

The pseudopotential approach is a simple calculation to be implemented numerically. It could investigate semiconductors features in less time. The results are less accurate than some ab initio methods though the approach is very helpful and still is used in the framework of the DFT method to render calculations more tractable.

Bibliography

[1] Richard m.martin, Electronic structure Basic Theory and Practical Methods,2004.

[2] L. P. Bouckaert, R. Smoluchowski, and E. Wigner, Phys. Rev. 50, 58 (1936) – "Theory of Brillouin zones and symmetry properties of wave functions in crystals".

[3] Hung-T Diep, Physique de la matière condensée, Dunod.

[4] P. Y. Yu and M. Cardona, Fundamentals of Semiconductors, Springer-Verlag, Berlin, 1999.

[5] C. Herring, Phys. Rev., 57 (1940) 1169.

[6]Empirical Pseudopotential Method: Theory and Implementation Details, Dragica Vasileska Professor, Arizona State University Tempe, AZ 85287-5706, USA.

[7] Optoelectronic properties of $ScxGa_1$-xN ternary alloys , Zouina Elbahi , university of djelfa , 2015.

[8] J.C. Phillips, Phys. Rev. 116 287 (1959).

[9] Bolland, Ian (2003) Complex band structure calculations of the electronic structure of nitride quantum wells, Durham theses, Durham University.

[10] M. L. Cohen and T. K. Bergstresser, Phys. Rev., 141 (1966) 789.

[11] G. Weisz, Phys. Rev. B, 149 504 (1966).

[12] A.O.E. Animalu, Phil. Mag., 13 53 (1966).

[13] S. Bloom and T.K. Berstresser, Solid State Commun, 6 465 (1968).

[14] J. R. Chelikowsky and M. L. Cohen, Phys Rev. B, 14 (1976) 556.

[15] Y. Yeo, C. Chong and M.F. Li, Appl. Phys. 83 1429 (1998).

[16] R. Coles, Theory of the electronic structure of quantum wells (PhD Thesis), Durham University (1998).

[17] O.Ambacher, J.Majewski, C.Miskys, A.Link, M.Hermann, M.Eickhoff, M.Stutzmann, F. Bernardini, V. Fiorentini, V. Tilak, B. Schaff and L.F. Eastman, J. Phys. Condens. Matter 14, 3399 (2002).

[18] S.K. Pugh, D.J. Dugdale, S. Brand and R.A. Abram, Semi. Sci. Tech., 14 23 (1999).

[19] L.M. Falicov and P.J. Lin, Phys. Rev. 141 562 (1966).

[20] Official documentation of LAPACK provider netlib "www.netlib.org/lapack/".

[21] Band Structure for Fourteen Semiconductors of the Diamond and Zincblende Structures Nicholas A. Mecholsky, The Catholic University of America Washington, DC, 20064.

[22] Measures from "https://www.mtixtl.com/bandgap-semiconductor.aspx".

Appendix

Code used for the calculation of the band structure

```
!-----------------------------------------------------------------
    program cohber
  !-----------------------------------------------------------------
  !
  ! program pour le calcul de la structure de bande
  ! pour les semiconducteurs diamand et zinc blende
  ! valeurs experimentaless pour les facteurs de forme selon Cohen
  ! and Bergstresser, PRB 141, 789 (1966)
  !     Expansion sur une base d'onde plane et diagonalisation
  !     Unites: hbar^2/2m = 1
  !     on utilise lapack dsyev et chetd2

  implicit none
  integer, parameter :: dp = selected_real_kind(14,200)
  !integer, parameter :: dp = kind(1.d0)
  !integer, parameter ::  cd=SELECTED_REAL_KIND(14,200).
  real(dp), parameter :: pi=3.14159265358979_dp, tpi=2.0_dp*pi
  !
  !    a  = parameter de reseau (a.u.)
  !    facreurs de forme en Rydberg
  !         x = symmetrique , a = antisymmetrique t
  !
  !
  real(dp), parameter ::  a=11.58, vs3=-0.21, vs8=0.02, vs11=0.06, &
                                  va3=0.06, va4=0.04, va11=0.02
  !    tau position des atomes (en unites de a)
  real(dp), parameter ::tau1=0.125, tau2=0.125, tau3=0.125
  !
  integer :: n, npw, npwx, nk
  real(dp) :: ecut, kg2, g2, vag, vsg, kg0(3), gij(3), h1(3), h2(3),
h3(3),&
              re,com,modu,b
  real(dp) ,allocatable :: a1(:,:),k(:,:), kg(:,:),e(:),d(:)&
                         ,eof(:)
  complex*8, allocatable :: h(:,:)
  complex*8, allocatable :: ta(:),work(:)
  integer :: i,j,m, nmax, n1, n2, n3, lwork, info,ii

  !
  !     on choisi : G_n=n*2pi/L, \hbar^2/2m*G^2 < Ecut

  open (11,file='kpoint.dat',status='unknown',form='formatted')
  !
  ! write (*,"hello")
  write (*,"('energy de coupure en Ry: ecut (Ry) > ',$)")
  read (*,*) ecut
  if ( ecut <= 0.0_dp) stop '  cutoff erroné '
```

```
  !
  !     Number and list of k-vectors
  !
  write (*,"('Nombre of k-vectors > ',$)")

read (*,*) nk
  if ( nk <= 0 ) stop ' parameter d entre erronés '
  allocate ( k(3,nk) )
  write (*,"('k (en 2pi/a units) > ')")
  do i=1, nk
      read (11,*, end=10, err=10)  k(1,i), k(2, i), k(3,i)
  end do
  10 continue
  !
  !  base de vecteurs pour le réseau réciproque en 2pi/a units
  !
  h1(1) = 1.0_dp;   h1(2) = 1.0_dp; h1(3) =-1.0_dp
  h2(1) = 1.0_dp;   h2(2) =-1.0_dp; h2(3) = 1.0_dp
  h3(1) =-1.0_dp;   h3(2) = 1.0_dp; h3(3) = 1.0_dp
  !
  !     boucle sur k-vectors
  !
    open (7,file='bands.out',status='unknown',form='formatted')

  !
  do n=1, nk
     !
     !    on compte les ondes plane tel que  (\hbar^2/2m)(k+G)^2 <
Ecut
     !    nmax est une estimation de l'indexe (voir memoire) ainsi on
génére
     !    les onde plane comme G(n1,n2,n3) =  n1*h1 + n2*h2 + n3*h3
     !
     nmax = nint ( sqrt (ecut) / (tpi/a * sqrt(3.0_dp) ) + 0.5 ) + 1
     npw = 0
     do n1 = -nmax, nmax
        do n2 = -nmax, nmax
           do n3 = -nmax, nmax
              !  k+G en 2pi/a units
              kg0(:) = k(:,n) + n1*h1(:) + n2*h2(:) + n3*h3(:)
              kg2 = (tpi/a)**2 * ( kg0(1)**2 + kg0(2)**2 + kg0(3)**2 )
              if ( kg2 <= ecut ) npw = npw+1
           end do
        end do
     end do
     print *, 'Nombre des ondes planes=',npw
     !
     allocate (kg(3,npw), e(npw), h(npw,npw),d(npw),&
               eof(npw),ta(npw),work(3*npw), a1(npw,npw))
     !
     !    on génére les ondes planes  (! en 2pi/a units)
     !
     i = 0
     do n1 = -nmax, nmax
        do n2 = -nmax, nmax
           do n3 = -nmax, nmax
kg0(:) = k(:,n) + n1*h1(:)+n2*h2(:)+n3*h3(:)
```

```
kg2 = (tpi/a)**2 * ( kg0(1)**2+ kg0(2)**2+ kg0(3)**2 )
if ( kg2 <= ecut ) then
                  i = i + 1
                  kg(:,i) = kg0(:)
               end if
            end do
         end do
      end do
      if ( i /= npw ) stop ' certaines ondes planes sont manquantes'
      !       cleanup
      h(:,:) =( 0.0_dp, 0.0_dp)
      !e(:)= 0.0_dp
      !eof(:)=0.0_dp
      !ta(:)=( 0.0_dp, 0.0_dp)
      !d(:)= 0.0_dp
      a1(:,:)= 0.0_dp
      !
      !    assigner les éléments de matrice du hamiltonien
      !       selon la base des ondes planes
      !
      do i=1,npw
         do j=1,npw
            gij(:) = kg(:,i) - kg(:,j)
            g2 = gij(1)**2 + gij(2)**2 + gij(3)**2
            if ( abs (g2-3.0_dp) < 1.0d-6 ) then
               vsg = vs3
               vag = va3
            else if ( abs (g2-4.0_dp) < 1.0d-6 ) then
               vsg = 0.0_dp
               vag = va4
            else if ( abs (g2-8.0_dp) < 1.0d-6 ) then
               vsg = vs8
               vag = 0.0_dp
            else if ( abs (g2-11.0_dp) < 1.0d-6 ) then
               vsg = vs11
               vag = va11
            else
               vsg =0.0_dp
               vag =0.0_dp
            end if
            if ( i ==j ) then
                re=(tpi/a)**2 * (kg(1,i)**2+kg(2,i)**2+kg(3,i)**2)+&
                vsg*cos(tpi*(gij(1)*tau1+gij(2)*tau2+gij(3)*tau3))
                com=vag*sin(tpi*(gij(1)*tau1+gij(2)*tau2+gij(3)*tau3))
                !re=dble(re)
                !com=dble(com)
                h(i,j)=cmplx(re,com )
              ! h(i,j) = ((tpi/a)**2 *
(kg(1,i)**2+kg(2,i)**2+kg(3,i)**2) +&
              !          vsg
               else
               re=vsg*cos(tpi*(gij(1)*tau1+gij(2)*tau2+gij(3)*tau3))
               com=vag*sin(tpi*(gij(1)*tau1+gij(2)*tau2+gij(3)*tau3))
```

```
                !re=dble(re)
                !com=dble(com)
                h(i,j)=cmplx(re,com)

               ! h(i,j) =( vsg *
cos(tpi*(gij(1)*tau1+gij(2)*tau2+gij(3)*tau3))&
                !        ,vag *
sin(tpi*(gij(1)*tau1+gij(2)*tau2+gij(3)*tau3)))
             end if
             !print  '(2i4,2f12.6)', i,j, h(i,j)
            !  0.0_dp
          end do
        end do
        !
        ! solution (les coefficients de developpement sont dans h(i,j)
        ! avec    j=sont fonction de indexe de base, i= fonction de
l'indexe de la valeur propre)
        !
        lwork = 3*npw


         ! conversion de la matrice hermitienne en matrice réelle
         call chetd2('U',npw,h,npw,d,eof,ta,info)

         do i=1,npw

         if(eof(i)< 1.0d-6)then
          eof(i)=0.0_dp
         endif
          if(d(i)< 1.0d-6)then
          d (i)=0.0_dp
         endif
         b=0.0_dp
         enddo
         !read(*,*)
         do i=1,npw
           do j=1,npw
           if ( i==j ) then
           a1(i,j)=real(h(i,j)) !d(i)
           print  '(2i4,2f12.6)', i,j, a1(i,j),d(i)
           else if(i==j-1) then
           a1(i,j)= real(h(i,j)) !eof(i)

             b= a1(i,j)*1.0_dp   !real(h(i,j)) !eof(i)
            print  '(2i4,2f12.6)', i,j, a1(i,j),eof(i)
            else if(i==j+1) then
            a1(i,j)=b
           print  '(2i4,2f12.6)', i,j,a1(i,j),b
          else
          a1(i,j)=0.0_dp !dble(0.0_dp)
           ! print  '(2i4,f12.6)', i,j, a1(i,j)
          endif
           !print  '(2i4,f12.6)', i,j, a1(i,j)
         enddo

         enddo
```

```
        !a1(:,:)= dble(h(:,:))
        call dsyev ( 'V', 'U', npw, a1, npw, e, work, lwork, info )



      if (info /= 0) stop ' diagonalisation de H-matrix a échoué '
      !
      write (*,'("k=",3f10.4)') k(:,n)
      write (*,'(4f12.4)') e(1:8)*13.6058
      !write(*,*)work(1)
      print  '(i4)',info

      !
      !  Ecrire le fichier de sortie et la relation de dispersion e(k)
      modu=sqrt (k(1,n)*k(1,n)+k(2,n)*k(2,n)+k(3,n)*k(3,n))


       write(7,*) modu, e(1:8)*13.6058        ! Energie en eV

      deallocate ( h, work, e, kg,a1,eof,d,ta)
      !
   end do
   close(7)

   stop

end program cohber
```